Title: Region-specific microRNA alterations in marmosets carrying SLC6A4 polymorphisms are associated with anxiety-like behavior.

Authors: Natalia Popa[1] PhD, Dipankar Bachar[1] PhD, Angela C. Roberts[2] PhD, Andrea M. Santangelo [2, ‡] PhD, and Eduardo Gascon [1,‡], MD, PhD.

[1] Aix Marseille Univ, CNRS, INT, Inst Neurosci Timone, Marseille, France

[2] Department of Physiology, Development and Neuroscience, University of Cambridge, Cambridge, United Kingdom

[3] Department of Physiology, Development and Neuroscience, Harvard University,

[‡] Co-senior authors

*Corresponding author: Eduardo Gascon, Institut de Neurosciences de la Timone, Aix-Marseille Université; CNRS UMR7289; 27, Boulevard Jean Moulin, 13005 Marseille (France); E-mail: eduardo.gascon-gonzalo@univ-amu.fr

Keywords: anxiety, marmoset, microRNA, ventro-medial prefrontal cortex, DCC

Running title: Marmoset SLC6A4 polymorphisms, anxiety and region-specific miRNAs

ABSTRACT

Human studies have consistently reported that stress-related disorders such as depression and anxiety impinge on the activity of emotion regulation networks including the ventromedial prefrontal cortex (vmPFC). However, molecular heterogeneity within the vmPFC and how these differences affect emotion regulation and behavior have not been elucidated. Marmosets have emerged as a powerful model in translational neuroscience to investigate molecular underpinnings of complex behaviors. Here, we took advantage of naturally occurring genetic polymorphisms in marmoset *SLC6A4* gene that have been linked to anxiety-like behaviors. Using FACS-sorted cells from different brain regions, we revealed that marmosets bearing different *SLC6A4* variants exhibit distinct miRNAs signatures specifically in neurons of vmPFC area 32, but not in those of closely related vmPFC area 25. We also identified DCC, a gene linked to anxiety and depression, as a downstream target of miRNAs deregulated in area 32. Significantly, we showed that levels of DCC and miRNAs in area 32 were highly correlated to anxiety-like behaviors as well as to the response to citalopram and 5-HT2a antagonists. Our findings establish links between genetic variants, molecular alterations localized to specific vmPFC regions and complex behavioral/pharmacological responses, providing new mechanistic insights into gene-behavior relationships underlying human psychopathology.

INTRODUCTION

Anxiety is a core symptom of multiple psychiatric disorders including depression and schizophrenia. A central goal in translational neuroscience is to better understand how aberrant brain function linked to such diseases arises from disruptions at the molecular level. It is widely accepted that anxiety stems from the evaluation of cost/benefits and/or the subsequent decision-making process (Corr *et al.*, 2021, Millan, 2003, Oathes *et al.*, 2015), functions that are highly dependent upon the prefrontal cortex (PFC). In particular, neuroimaging studies in humans have linked ventromedial PFC (vmPFC) activity in cost-benefit decisions (Talmi *et al.*, 2009, Tom *et al.*, 2007) and in emotional responses under conflict situations (Egner *et al.*, 2008, Hiser and Koenigs, 2018). Similarly, whilst decision variables appear widely represented across the frontal cortex of macaque monkeys (Kennerley *et al.*, 2009, Mehta *et al.*, 2019), neurons in the vmPFC have been specifically identified to encode the gain or cost associated with expected outcomes (Haroush and Williams, 2015, Hayden and Platt, 2010, Kennerley *et al.*, 2009) as well as their emotional valence (Amemori and Graybiel, 2012, Amemori *et al.*, 2015). Not surprisingly then, altered processing and deficiencies in vmPFC circuitry have been implicated in the enhanced negative emotion typical of anxiety and affective disorders (Hiser and Koenigs, 2018, Via *et al.*, 2018). Moreover, vmPFC activity not only predicts treatment efficacy but its normalization parallels remission (Kennedy *et al.*, 2007, Fox *et al.*, 2012) . It is important to recognize, however, that the vmPFC encompasses distinct regions with marked differences in cellular composition, connectivity patterns and function (Hiser and Koenigs, 2018, Roberts and Clarke, 2019, Myers-Schulz and Koenigs, 2012, Stawicka *et al.*, 2020, Wallis *et al.*, 2019, Zeredo *et al.*, 2019).

Of particular relevance to the vmPFC's involvement in the etiology and treatment of anxiety are its particularly high levels of the serotonin transporter, compared to the rest of the PFC (Way *et al.*, 2007). Selective serotonin reuptake inhibitors that target the transporter are the first line treatment for anxiety and depression (Goodman, 2004) and genetic variants in the *SLC6A4* gene (encoding the serotonin transporter) (Lesch *et al.*, 1996) or HTR1A (Lemonde *et al.*, 2003, Strobel *et al.*, 2003) are linked to a higher risk of anxiety and depression. Thus, understanding the cellular mechanisms by which serotonin regulates vmPFC function will help in the quest for more rational therapeutic targets for the treatment of anxiety. MicroRNAs (miRNAs) are attractive candidates as they have been shown to modulate such regulatory neurotransmitters and signaling cascades and to be de-regulated in patients with affective disorders (for review see (Allen and Dwivedi, 2020, Lopez *et al.*, 2018). They are a class of short (20-25 nt) non-coding RNAs and one of the best-studied posttranscriptional modifiers of gene expression (Huntzinger and Izaurralde, 2011, Izaurralde, 2015). miRNAs repress expression of messenger RNAs (mRNAs) containing complementary sequences and have been involved in multiple pathological processes, including psychiatric diseases (Geaghan and Cairns, 2015, Yoshino and Dwivedi, 2020). In particular, the investigation of miRNAs in psychiatric disorders has gained momentum as accumulating evidences indicate that miRNAs could potentially be used as biomarkers and/or therapies (Belzeaux *et al.*, 2017, Roy *et al.*, 2020).

The common marmoset, *Callithrix jacchus*, has emerged as a reference model in modern neuroscience. Compared to rodents, marmosets are closer to humans, not only in their behavioral repertoire and brain organization, including vmPFC, but also in molecular terms (Finkenwirth *et al.*, 2015, Miller *et al.*, 2016). Recent studies in this

species have thus shown that, similar to humans, *SLC6A4* polymorphisms affect the regulation of behaviors elicited by threat in the human intruder paradigm, the response to antidepressants and the neurochemical balance in brain areas implicated in emotional processing (Santangelo *et al.*, 2016, Santangelo *et al.*, 2019). In addition, recent studies have revealed distinct functional units within marmoset vmPFC in relation to emotion regulation (Alexander *et al.*, 2019, Alexander *et al.*, 2020, Roberts and Clarke, 2019, Wallis *et al.*, 2017). To directly assess gene-behavior relationships in a primate, we used marmosets carrying distinct *SLC6A4* haplotypes as the experimental model to dissect out molecular (namely in miRNAs) alterations linked to trait-like anxiety, within distinct regions of vmPFC. We revealed that *SLC6A4* variants were related to miRNA alterations in a remarkably region-specific manner. We also identified DCC, a gene previously implicated in affective disorders, as a downstream target of the deregulated miRNA networks. Since such changes were highly correlated to behavioral responses, our results underscore the intimate link between molecular differences among vmPFC areas and complex behavioral outcomes, thereby providing mechanistic insights into gene-behavior interactions and the neurobiology of emotion regulation.

MATERIALS AND METHODS

Subjects

For this study 6 adult male common marmosets, Callithrix jacchus, (26 ± 2 mo, 413 ± 17 g) balanced for SLC6A4 genotype were used in this study (Supplementary table 1). All animals had MRI and [18F]altanserin PET scans, human intruder (HI) test, and snake testing (procedures described previously by (Shiba *et al.,* 2014)) before entering a pharmacological study, which consisted of repeated HI test with acute intramuscular (i.m.) doses of citalopram (behavioral data reported elsewhere (Santangelo *et al.,* 2016)) and, after 2 months, with the 5HT2A antagonist M100907 (Santangelo *et al.,* 2019) .

Marmosets were bred onsite at the Innes Marmoset Colony (Behavioral and Clinical Neuroscience Institute) and housed as male-female pairs (males were vasectomized). Temperature (24 °C) and humidity (55%) conditions were controlled, and a dawn/dusk-like 12-h period was maintained. They were provided with a balanced diet and water ad libitum. This research has been regulated under the Animals (Scientific Procedures) Act 1986 Amendment Regulations 2012 following ethical review by the University of Cambridge Animal Welfare and Ethical Review Body.

Behavioral testing

The human intruder test involves measuring the animal's behavioral response to an unfamiliar human, the "human intruder," who stands in front of the animal's home-cage and maintains eye contact with the animal. Since animals bred in the laboratory have prior positive and negative experiences with human encounters, e.g., receiving food treats or being restrained for husbandry or experimental purposes, the unfamiliar "human intruder" acts as a threat with low probabilistic imminence and creates an

anxiety-provoking context. Avoidance and vigilance during the task are similar to human anxious behavior and sensitive to anxiolytics (Carey *et al.,* 1992).

The procedure for the human intruder test is based on the method used by (Santangelo *et al.,* 2016). Cameras and microphones are routinely present in the room for recording purposes such that all animals are habituated to the presence of recording equipment. Before the testing session begins, a camera and microphone are set up in front of the animal's home-cage. The animal was tested in the top-right quadrant of their home cage. During testing, the cagemate was separated from the subject and restricted to the left half of the home cage and was obscured from both the human intruder and the subject. After 8 min of being separated, an experimenter (unfamiliar to the animal) wearing a realistic latex human mask (Greyland Film, UK) and standard lab attire stood 40 cm from the cage and maintained eye contact with the subject for 2 min (intruder phase). Recording continued for a further 5 min after the intruder left (recovery phase). Behavior and vocalizations during the intruder phase were scored.

The model snake test involves recording the animal's behavioral response to a rubber snake which acts as an inherent predatory stimulus, provoking an innate fear response (Barros *et al.,* 2000). Furthermore, as the model snake is placed directly within the homecage, the model snake presents far higher spatial threat imminence compared to the intruder in the human intruder test (Mobbs *et al.,* 2020).

The procedure of the model snake test is based on the methods in (Shiba *et al.,* 2014). Before the testing session begins, wireless cameras and a microphone are placed to record the animal's behavior from a top-down view and a frontal view. During a test session, the animal is separated from their cagemate and restricted to the upper right quadrant of their home cage, while the cagemate was separated by opaque dividers

to the left half of the home cage and cannot see into the testing quadrant. The 20-min test session is divided into four 5-min phases: a separation phase, where only the camera and microphone were present; a pre-snake phase, where an empty box without the model snake (a 27 cm tall rubber model of a rearing cobra) is placed in the test quadrant; a snake phase, where the empty box from the previous phase is replaced with a box containing the model snake (a sliding door is removed to expose the model snake once the box is in position); and a post-snake phase, where the empty box from the pre-snake phase is re-introduced into the test quadrant. Analyzed behaviors are summarized in Supplementary Table 2.

Pharmacological Manipulation on the intruder test

Six homozygous marmosets were included in this study. Animals were injected i.m. with citalopram (10 mg/kg), with the selective 5-HT2A antagonist M100907 (Sigma–Aldrich) (0.3 mg/kg) or vehicle (0.01 M PBS-HCl) 25 min before the intruder phase. Procedures for the human intruder test were exactly the same as described above. To avoid habituation to the human intruder across sessions the intruder wore different realistic rubber human masks each session. The experimental design was a latin square randomized by sex, genotype, and masks. Treatment order was the same for all individuals (lower dose, higher dose, and vehicle) with 2 weeks between each session.

Genotyping

Genomic DNA (gDNA) was extracted from hair follicles of the back of the animals using using the QIAamp DNA Micro kit for forensic casework samples (Qiagen) (yield

0.5–1.2 µg per sample). Primers were designed to flank the SLC6A4 repeat region (Supplementary Table 3). HotStarTaq Plus DNA Polymerase (Qiagen) was used in a BioRad C1000 thermal cycler (conditions: activa- tion 15min at 94°C; 44 cycles of 30s at 94°C, 30s at 55°C and 1 min at 72 °C; and termination 5 min at 72 °C). The PCR product was visualized in an agarose gel, purified using the Mini Elute PCR Purification Kit (Qiagen) and sent for sequencing (Source BioScience, Cambridge, UK). Primers used for sequencing can be found in Supplementary Table 3.

Sample preparation

At the end of the study, animals were premedicated with ketamine hydrochloride before being euthanized with pentobarbital sodium (Dolethal; 1 mL of a 200-mg/mL solution; Merial Animal Health). Brain were dissected, frozen using liquid nitrogen, and then sliced in a cryostat at −20 °C to 200-µm-thick sections. Tissue samples for each target region were excised using punches of 1.0 and 1.5-mm radio length. Eight punches per target region were used in this study (4 from the right hemisphere and 4 from the left hemisphere).

Nuclei isolation and sorting

8 punches/area/animal were used. Nuclei extraction protocol was adapted from Halder et al. (2016). All steps were performed at 4 °C or on ice. Tissues were homogenized in nuclei isolation buffer (0.32 M Sucrose, 10 mM HEPES pH 8.0, 5 mM $CaCl_2$, 3 mM $Mg(CH_3COO)_2$, 0.1 mM EDTA, 1 mM DTT, 0.1% Triton X-100) with a 2 ml Dounce homogenizer by 10 gentle strokes with each pestle and filtered through a 40 µm strainer. After centrifugation, nuclei pellets were resuspended in 1 ml PBS-RI (PBS, 50 U/mL Rnase-OUT Recombinant Ribonuclease Inhibitor (Invitrogen), 1 mM DTT)

and fixed by the addition of 3 ml PBS 1.33% paraformaldehyde (Electron Microscopy Sciences) for 30 minutes on ice. Fixed nuclei were spun down, washed with 1 ml PBS 0.1% triton-X-100, pelleted again and resuspended at 10^6 nuclei per ml in stain/wash buffer (PBS-RI, 0.5% BSA, 0.1% Triton-X-100) containing 2 µg/ml anti-NeuN-alexa-488 antibody (Millipore, MAB377X) and 1 µg/ml Hoechst 33342 (Molecular Probes). After 30 minutes incubation on ice protected from light, nuclei were washed with 2 mL stain/wash buffer and spun down. Finally, stained nuclei were resuspended in 1 ml PBS-RI 0.5% BSA and filtered again through a 40 µm strainer. Nuclei suspensions were maintained on ice protected from light until sorting.

Sorting of nuclei was achieved with a MoFlo Astrios EQ Cell sorter (Beckman Coulter). After positive selection of intact Hoechst-positive nuclei and doublets exclusion, all NeuN-positive and NeuN-negative nuclei were separately isolated. Sorted nuclei were collected in refrigerated 2 ml microtubes containing 0.5 ml PBS-RI 0.5% BSA. Finally, nuclei were spun down, supernatants eliminated and pellets were conserved at -80°C untill RNA extraction.

RNA extraction and reverse transcription

Total RNAs (small and large RNAs) were extracted in one fraction with miRNeasy FFPE kit (Qiagen) following manufacturer's protocol with minor changes. Briefly, nuclei pellets were lysed in 150 µL PKD buffer and 10 µl proteinase K for 15 minutes at 56°C, then immediately incubated at 80°C for 15 minutes in order to reverse formaldehyde modification of nucleic acids and then immediately incubated 3 minutes on ice. After centrifugation, supernatants were transferred in new 2 ml microtubes and remaining DNA was degraded during a 30 minutes incubation with DNase Booster Buffer and DNase I. Addition of RBC buffer and ethanol allowed RNA binding to MiniElute spin

columns. After washing steps, pure RNAs were eluted with 20 µl of RNase-free water. Total RNA concentrations were determined with a Nanodrop spectrophotometer (Fisher Scientific).

miRNA reverse transcription and quantification

miRNAs were specifically reverse transcribed with TaqMan Advanced miRNA cDNA Synthesis Kit (Applied Biosystems). Depending on RNA concentration, 10 ng or 2 µl total RNA were used as starting material for each poly(A) tailing reaction, followed by adaptor ligation and reverse transcription. We chose not to perform the last pre-amplification reaction in order to avoid eventual amplification bias.

The expression level of 752 miRNAs was screened by real-time PCR with TaqMan Advanced miRNA Human A and B Cards (Applied Biosystems A31805). cDNAs were diluted 1:10 with 0.1X TE buffer, then mixed with water and TaqMan Fast Advanced Master Mix 2X (Applied Biosystems) and 100 µL of this mix was loaded in each fill reservoir of two array cards. Real-time PCR reactions were run on a QuantStudio 7 Flex Real-Time PCR System (Applied Biosystems).

mRNA reverse transcription and quantification

40 ng total RNAs were reverse transcribed with SuperScript IV Reverse Transcriptase (Invitrogen) and random hexamers in 30 µl total reaction volumes. cDNAs were diluted with water and 266 pg of cDNA was used in each 20 µl-PCR reaction in 96-well plates. Gene expression was quantified by real-time PCR with marmoset specific TaqMan Gene Expression Assays (Applied Biostems) and TaqMan Fast Advanced Master Mix (Applied Biosystems) on a QuantStudio 7 Flex Real-Time PCR System (Applied Biosystems).

Data analysis

Data were revised and analyzed using ThermoFisher Scientific Digital Science online tools (thermofisher.com/fr/en/home/digital-science.html). Relative quantification was performed with the ΔΔCt method.

368 miRNAs were robustly amplified and were considered for subsequent analysis. DeltaCt values were obtained by global normalization method. qPCR results were first normalized (using global mean normalization method) and then transformed to relative expression levels via the 2^{-DCt} equation.

Four references genes were used as endogenous control genes (POLR2A, TBP, HPRT1, PGK1). DeltaCt values were obtained by subtracting the mean Ct value of these 4 control genes to the Ct value of each target gene.

For behavioral experiments, EFA in HI test or snake model tests were extracted as previously described (Quah *et al.,* 2020).

Statistics

All values were represented as scatterplot with the mean ± SEM. Statistical analysis was performed using XLStat (PCA), GraphPad 7.0 (ANOVA, correlation analysis and t-tests) and R (PCA and regression analysis). A significance threshold of a 0,05 was used in all experiments.

Statistical differences between two groups were analyzed with Student's t tests. Correlations were calculated using the Pearson correlation coefficient with 2-tailed analysis. Otherwise, 1- or 2-way analyses of variance were performed. No statistical methods were used to determine the sample sizes, but the number of experimental subjects is similar to sample sizes routinely used in our laboratory and in the field for

similar experiments. All data were normally distributed and variance was similar between groups, supporting the use of parametric statistics. Statistical differences were set to $p<0.05$.

RESULTS

microRNA profiling in the marmoset cortex discriminates between NeuN$^+$ and NeuN$^-$ cells across cortical areas

In order to investigate whether miRNAs signatures could be linked to behavioral responses, we first validated an experimental approach previously applied to human samples (Lutz *et al.,* 2017) (Fig. 1a). Brains from genotyped and behaviorally phenotyped marmosets were sliced and punches from selected brain regions were harvested. After nuclear isolation, samples were FACS sorted into NeuN$^+$ and NeuN$^-$ cells (Suppl. Fig. 1a) and RNA extracted from each fraction. As expected, NeuN$^+$ cells are enriched in neuron-specific markers (Grm7, Gabra1, Camk2) and deprived almost entirely of glial-associated genes (astrocyte, oligodendrocytes and microglia markers, Fig. 1b and Suppl. Fig. 1b). In contrast, NeuN$^-$ cells express strong levels of astrocytes (Gfap, Aldh1l1 or Slc1a3), oligodendrocytes (Klk6, Plp1, Cnskr3) and microglial genes (Aif1) (Fig. 1B and Suppl. Fig. 1b). We also observe a low expression of neuronal genes in this fraction as it is known that a subset of neurons of the primate cortex are NeuN$^-$ (Lutz *et al.,* 2017). Similar profiles were obtained in samples from different cortical regions (area 17, 25 and 32) indicating that FACS sorting is a reliable method to enrich neurons from different marmoset cortical areas for transcriptomic analysis.

Although miRNA expression in different brain cell types remains largely unexplored, we hypothesize that, given the differences in cell composition, miRNAs signatures present in NeuN$^+$ and NeuN$^-$ populations should be dramatically distinct. Using miRNA quantitative PCR, we profiled 754 miRNAs in our samples and found that almost 100 miRNAs were consistently expressed in both subpopulations. Using these miRNAs,

we performed a principal component analysis (PCA) in NeuN$^+$ and NeuN$^-$ nuclei coming from 6 different marmosets. As shown in Fig. 1c, NeuN$^+$ and NeuN$^-$ samples formed separated clustered across the PC1 axis confirming that, even considering only those miRNAs whose expression is shared, miRNAs profiles readily distinguish both fractions.

Recent work (Krienen *et al.,* 2020) revealed important regional differences in gene expression across the marmoset cortex. We next investigated whether, similarly, miRNA profiling might be sensitive enough and detect such regional variations. For that purpose, we examined 3 cortical areas; on one hand, we profiled the primary visual cortex (corresponding to Brodmann area 17) as an example of sensory region endowed with specific cytoarchitectonic and functional features (e.g. expanded layer IV, strong myelination, major inputs from the thalamus). On the other hand, we considered two high-order association areas within the vmPFC (Brodmann area 25 and 32) whose activity has been shown to be consistently deregulated in affective disorders (Egner *et al.,* 2008, Etkin *et al.,* 2006). PCA on miRNA levels (154 miRNAs that are consistently detected in all NeuN$^+$ samples) from these different areas enabled reconstruction of such regional pattern in NeuN$^+$ cells (Fig. 1d) but not in NeuN$^-$ cells (Suppl. Fig. 1c). Samples from the visual cortex clustered together on one side of the PC1 axis indicating a clear segregation between sensory and association areas in terms of miRNAs signature. In contrast, the two regions of the PFC appeared intermingled. Accordingly, a number of miRNAs (Suppl. Fig. 1d) are differentially expressed in the visual cortex. Again, such regional pattern cannot be observed in the NeuN$^-$ fraction (Suppl. Fig. 1c) suggesting that anatomo-molecular differences largely

arise from neurons. Together, these findings support the notion that miRNAs profiling is a powerful method to uncover molecular differences in the brain.

microRNA profiling uncovers region-specific molecular differences in marmosets bearing different SLC6A4 variants/haplotypes

Genetic polymorphisms in the marmoset *SLC6A4* promoter region have been linked to high trait anxiety (Santangelo *et al.,* 2016). Since primate vmPFC has been widely involved in emotional processing (Roberts and Clarke, 2019), we sought to determine whether miRNA profiling could unveil molecular differences in marmosets bearing the two most frequent *SLC6A4* haplotypes (AC/C/G versus CT/T/C) described previously [34]. For that purpose, we analyzed miRNAs contents in 3 marmosets for each variant. As depicted in Fig. 2a, PCA on NeuN$^+$ neurons showed two independent clusters in area 32 corresponding to each genotype suggesting that this region might be specifically affected by *SLC6A4* polymorphisms. No such pattern was observed either in the primary visual cortex or in area 25, arguing against a broad cortical effect of the polymorphism. In order to confirm this genetic effect, we carried out a 2-way ANOVA on the miRNA levels in each region. We found that area 32 exhibited a significant effect of genotype on the miRNA expression ($F(1, 4)=17.06$; $p=0.0145$) whereas this was not observed in areas 17 ($F(1, 4)= 2.419$; $p=0.1949$) and 25 ($F(1, 4)=0.1311$; $p=0.1311$).

To determine which miRNAs are significantly and specifically deregulated in area 32 (differentially expressed miRNAs, DEmiRs), we took into account our results from the PCA and considered a list of 25 miRNAs that contributed the most to the first two PCs

(Table 1). miRNAs that exhibited differential expression in area 32 but not in BA17 and 25 are shown in Fig. 2b.

To confirm the specificity of this observations, we also analyzed the expression of neuronal miRNAs associated with visual cortex. Although a number of miRNAs (miR-195, miR-221, miR-222 and miR-497) were found to be differentially expressed in the visual cortex compared to area 25 and 32 (Suppl. Fig. 2), none of the BA17 DEmiRs showed any difference across the genotypes, suggesting that there exist miRNAs whose expression is altered in precise regions in a genotype-dependent manner. Overall, our observations confirm that miRNAs could reliably uncover molecular differences in the marmoset cortex and indicate *SLC6A4* polymorphisms selectively alter miRNA signatures in area 32.

Genotype-specific changes of DCC expression in area 32

miRNAs regulate gene expression post-transcriptionally. We reasoned that miRNAs alterations in area 32 would result in significant changes in downstream target transcripts. To identify those targets and thus further validate our miRNAs signatures, we carried out a network analysis of the area 32 deregulated miRNAs using miRNet (Chang *et al.,* 2020) (Fig 3a). We restricted our analysis using two criteria: i) target genes bearing binding sequences for, at least, three of the miRNAs differentially expressed in area 32 across *SLC6A4* variants; and ii) a coefficient correcting for miRNA abundance. Thus, we profiled the expression of 20 target genes as well as 15 control transcripts in area 25 and 32. None of the target mRNAs show significant changes in area 25 (Suppl. Fig. 3). In contrast, in area 32, DCC, was found to be differentially expressed across *SLC6A4* genotypes. DCC is the netrin receptor and recent work has

associated their expression in the prefrontal cortex to depression and anxiety (Li *et al.*, 2020, Manitt *et al.*, 2013, Torres-Berrío *et al.*, 2017, Torres-Berrío *et al.*, 2020). DCC transcript contains putative sequences for miR-9-5p, let7-5p and miR-190. Levels of DCC were reduced in CT/T/C marmosets and inversely correlated to the levels of BA32-deregulated miRNAs (higher in CT/T/C animals, Fig. 2b). Despite the number of miRNA sequences present in DCC mRNA, the observed downregulation was moderate, in agreement with the contention that miRNAs fine-tune gene expression (Torres-Berrío *et al.*, 2020, Torres-Berrío *et al.*, 2020). Finally, we observed no reduction of DCC in area 25 (Suppl. Fig. 3) and no alteration of the reference transcripts in either BA25 or 32. Overall, our findings argue again for the anatomical specificity of molecular alterations associated with *SLC6A4* polymorphisms.

Molecular alterations in area 32 correlate with behavioral response to uncertain threat

It has been previously shown that *SLC6A4* polymorphisms strongly influence anxiety-like behavior in response to uncertainty in the human intruder test (HI-test), but do not alter evoked fear-like behavior in the more certain context of the snake test (ST) (Quah *et al.*, 2020, Santangelo *et al.*, 2016). Using exploratory factor analysis (EFA), a recent study demonstrated that a single factor in the EFA explained behavior on the HI test whereas two factors were necessary to describe behaviors elicited on the ST (Quah *et al.*, 2020).

We reasoned that, if relevant, the molecular alterations identified in area 32 might correlate with behavioral responses in the anxiety-related HI-test but not the fear-related snake test. We therefore performed a correlation analysis on the levels of miRNAs deregulated with the EFA score for HI-test. We observed a significant

negative correlation for four miRNAs in area 32 (Fig. 4a), showing a R^2 coefficient ranging from 0.45 to 0.94; miR-525-3p showed the strongest association with an R^2=0.94 (p=0.0013), followed by miR-125b-5p (R^2=0.78; p=0.0197), let-7d-5p (R^2=0.69; p=0.0393) and miR-125a-5p (R^2=0.68; p=0.0407). Remarkably, DCC contents also showed a significant but inverted correlation to the behavioral score (R^2=0.899; p=0.0039). In contrast, levels of the same miRNAs and DCC in area 25 exhibited no correlation with the HI test EFA (Fig. 4) arguing for the specificity of our findings. Moreover, the two behavioral scores in the ST were also not correlated with any of these miRNAs in area 32 (Suppl. Fig. 4) supporting the notion that the molecular alterations we found in area 32 are connected to the differential behavioral response to uncertain threat in marmosets bearing the different *SLC6A4* variants.

Finally, recent work has suggested that the effectiveness of anxiolytics, including serotonin reuptake inhibitors and 5-HT2a receptor antagonists to dampen anxiety-behavior towards the intruder differs in marmosets homozygous for AC/C/G versus CT/TC variants (Santangelo *et al.*, 2016, Santangelo *et al.*, 2019). We asked whether these differential responses to citalopram (10 mg/kg) or the selective 5-HT2A antagonist, M100907 (0.3 mg/kg) were significantly correlated with miRNAs levels. We focused on the average distance the animals moved in response to the human intruder as this parameter is influenced by both pharmacological treatments. As shown in Fig. 5, whilst only miR-9-5p levels in area 32 were specifically associated with the citalopram response (R^2=0.8026; p=0.0157), M100907 effects were correlated instead with those of miR-525-3p (R^2=0.8808; p=0.0056). No miRNAs in area 25 showed any correlation with the responses to citalopram or M100907 treatment supporting the anatomical segregation of molecular changes (Suppl. Figure 5). Together, these observations

reveal the intimate links between area 32 molecular composition (specific miRs and DCC) and its function in the elaboration of complex behavioral responses towards uncertain threats.

DISCUSSION

Using a novel approach to investigate miRNA signatures in marmosets, we reveal specific molecular alterations within distinct regions of the vmPFC that underlie anxiety-related *SLC6A4* polymorphisms. Focusing on miRNAs in areas 32 and 25, with primary visual area 17 acting as a control region, we show that: i) miRNAs are dramatically different across cell types and cortical regions; ii) *SLC6A4* polymorphisms impinge selectively on miRNA signatures in area 32; iii) levels of specific miRNAs as well as of the target gene, DCC, correlate with anxiety-like behavior in response to uncertain threat in the intruder test; and iv) the responsiveness of such anxiety-like behavior to anxiolytics is also associated with specific miRNAs. Although based on a limited number of samples, our results highlight the exquisite refinement of behavioral-molecular correlations.

The paucity of appropriate experimental models has precluded anatomical and molecular investigation of vmPFC in anxiety-like behaviors. Marmosets have emerged as an attractive model in translational neuroscience (Miller *et al.*, 2016, Oikonomidis *et al.*, 2017). On one hand, previous work has clearly demonstrated that naturally occurring polymorphisms in the *SLC6A4* promoter region are linked to anxious-like behaviors (Santangelo *et al.*, 2016, Santangelo *et al.*, 2019), similar to that reported in humans (Lesch *et al.*, 1996, Wilkie *et al.*, 2009). On the other hand, marmoset vmPFC parcellation appears to be markedly similar to that found in humans (Roberts and Clarke, 2019, Schaeffer *et al.*, 2020). Although both peri- and subgenual cortex have been consistently implicated in threat processing and stress-related disorders, it has been difficult to establish their functional differences. A recent study (Ironside *et al.*, 2020)

used a common approach-avoidance task in macaques and humans (both healthy controls and depressed patients) to compare fMRI data. Interestingly, this work highlighted a shared primate network for aversive behavior. This circuit involved the perigenual ACC (area 32) and was deregulated in depressed patients. In the marmoset, direct comparison of area 25 and 32 has revealed their functional differentiation in threat reactivity, not only in relation to approach-avoidance decision making but also in the extinction of Pavlovian conditioned threat responses (Wallis *et al.,* 2019). However, while overactivation of area 25 specifically evokes anxiety-like behavior in response to uncertainty evoked in the HI threat test (Alexander *et al.,* 2020), the involvement of area 32 has not yet been addressed. In light of our findings, future experiments using opto/chemogenetics in marmosets should precisely delineate the contribution of each area in the HI test.

From a molecular perspective and in line with recent single-cell RNA data (Hodge *et al.,* 2019, Krienen *et al.,* 2020), we provide experimental evidence for the existence of distinct miRNA signatures in specific cortical areas of the marmoset brain. Importantly, we reveal changes in this miRNA profile selectively in vmPFC area 32 related to an SLC6A4 polymorphism, of particular relevance to our understanding of the neurobiological mechanisms underlying gene-behaviour relationsips. The repertoire of non-coding RNAs (ncRNAs) has expanded across evolution and multiple studies support the notion that primate-restricted ncRNAs contribute to psychiatric conditions including depression (Issler *et al.,* 2020, Lopez *et al.,* 2014). Building on these findings, our results reveal a primate-specific miRNA, miR-525-3p, the levels of which are best correlated with uncertainty-evoked anxiety-like behavior. miR-525 is an evolutionary recent miRNA as shown by the exact sequence conservation between human, gorilla,

and chimpanzee. A less conserved sequence is found in other old-world (orangutan, baboon and macaques) and new-world monkeys (marmosets and squirrel monkeys) but not in prosimians (mouse lemur) suggesting that a common miR-525 ancestor appeared about 40 million years ago (Suppl. Fig. 6). Together, these results highlight the importance of molecular investigations in the brains of primates that have the potential to uncover evolutionary recent molecular pathways of utmost interest for translational psychiatry.

We also showed that miRNA alterations in area 32 regulate the expression of DCC. DCC is the cognate receptor for netrin, a guidance cue involved in axon navigation during development (Tessier-Lavigne and Goodman, 1996). Remarkably, mutations in human *DCC* have been linked to human pathology (Srour *et al.*, 2010), including stress-related disorders (Li *et al.*, 2020, Manitt *et al.*, 2013, Torres-Berrío *et al.*, 2017). As previously described (Rajman and Schratt, 2017, Schratt, 2009), changes in miRNAs led only to a modest reduction of DCC mRNA. Nonetheless, miRNA-dependent fine-tuning of specific targets has been consistently involved in the physiopathology of stress-related disorders (Fiori *et al.*, 2020, Lopez *et al.*, 2017, Torres-Berrío *et al.*, 2017). Moreover, it has been shown that DCC expression in the prefrontal cortex is particularly high during adolescence and that DCC levels contribute to vulnerability to stress-related disorders in mice (Torres-Berrío *et al.*, 2020, Torres-Berrío *et al.*, 2020). Here, we present novel evidence that miRNAs fine-tune DCC contents in a region-dependent manner (Fig. 3 and Suppl Fig 3) and that DCC regulation may be essential for the normal functioning of specific vmPFC circuits (Fig. 4 and Suppl Fig 4). Human studies have already implicated some of the miRNAs identified here, such as miR-9-5p or let-7d-5p, in psychiatric conditions (Camkurt *et al.*, 2020, He *et al.*, 2021, Maffioletti

et al., 2016) and work in rodents have provided causal evidence confirming such links (Bahi and Dreyer, 2018, Ma *et al.*, 2019, Zhang *et al.*, 2020). The current results pave the way for future work to identify the cellular mechanisms by which *SLC6A4* variants alter miRNAs and DCC levels in selective cortical areas.

In summary, miRNAs are short molecules endowed with an enormous interest for translational psychiatry (Lopizzo *et al.*, 2019, Zhou *et al.*, 2021). Here, we have identified a set of miRNAs whose levels are correlated to different behavioral outcomes in response to uncertainty measured by the HI test, a paradigm ethologically relevant for the investigation of stress-related disorders (Roberts, 2020). The finding that a SLC6A4 polymorphism related to vulnerability to trait anxiety in humans is associated with localized changes in miRNAs within vmPFC in marmosets is highly relevant to our understanding of psychiatric diseases (Lopez *et al.*, 2014, Roy *et al.*, 2020). It also sheds light onto the molecular control of threat-processing networks. Accumulating evidence indicates that miRNAs could be useful biomarkers to evaluate the responsiveness to antidepressants (Labermaier *et al.*, 2013, Lopez *et al.*, 2018). Our observations expand this notion and suggest that specific miRNAs could be related to distinct pharmacological pathways. Thus, miR-9 levels correlate with the effects of citalopram on threat responsivity while miR-525 levels predict the threat responsivity effects of 5-HT2a antagonists (Fig. 5). The influence of genetic variants on the levels of these miRNAs in a region-specific manner revealed here, highlight the need to integrate genetic, molecular, imaging and clinical data for personalized therapy.

FUNDING AND DISCLOSURE STATEMENT

This work was supported by France National Agency (ANR18-CE37-0017), NRJ foundation, Celphedia and Fondation de France (00100077) to EG and a Wellcome Trust Investigator award (108089/Z/15/Z) to A.C.R.

The authors report no biomedical financial interests or potential conflicts of interest.

AUTHOR CONTRIBUTIONS

ACR, AMS and EG conceived and designed the project. AMS performed the behavioral testing and sample preparation. NP performed miRNA and gene expression experiments. NP, AMS, DB and EG analyzed the data. ACR provided contribution to the interpretation of data. AMS, ACR and EG wrote the manuscript. NP, ACR, AMS and EG discussed the results, reviewed and edited the final manuscript.

ACKNOWLEDGEMENTS

We would like to thank Stephane Robert from the AMUTICYT facility for his precious support for the FACS sorting. We also thank Catherine Lepolard for technical help.

REFERENCES

1. Corr R, Pelletier-Baldelli A, Glier S, Bizzell J, Campbell A, Belger A (2021). Neural mechanisms of acute stress and trait anxiety in adolescents. *Neuroimage Clin* **29**: 102543.
2. Millan MJ (2003). The neurobiology and control of anxious states. *Prog Neurobiol* **70**: 83-244.
3. Oathes DJ, Patenaude B, Schatzberg AF, Etkin A (2015). Neurobiological signatures of anxiety and depression in resting-state functional magnetic resonance imaging. *Biol Psychiatry* **77**: 385-393.
4. Talmi D, Dayan P, Kiebel SJ, Frith CD, Dolan RJ (2009). How humans integrate the prospects of pain and reward during choice. *J Neurosci* **29**: 14617-14626.
5. Tom SM, Fox CR, Trepel C, Poldrack RA (2007). The neural basis of loss aversion in decision-making under risk. *Science* **315**: 515-518.
6. Egner T, Etkin A, Gale S, Hirsch J (2008). Dissociable neural systems resolve conflict from emotional versus nonemotional distracters. *Cereb Cortex* **18**: 1475-1484.
7. Hiser J, Koenigs M (2018). The Multifaceted Role of the Ventromedial Prefrontal Cortex in Emotion, Decision Making, Social Cognition, and Psychopathology. *Biol Psychiatry* **83**: 638-647.
8. Kennerley SW, Dahmubed AF, Lara AH, Wallis JD (2009). Neurons in the frontal lobe encode the value of multiple decision variables. *J Cogn Neurosci* **21**: 1162-1178.
9. Mehta PS, Tu JC, LoConte GA, Pesce MC, Hayden BY (2019). Ventromedial Prefrontal Cortex Tracks Multiple Environmental Variables during Search. *J Neurosci* **39**: 5336-5350.
10. Haroush K, Williams ZM (2015). Neuronal prediction of opponent's behavior during cooperative social interchange in primates. *Cell* **160**: 1233-1245.
11. Hayden BY, Platt ML (2010). Neurons in anterior cingulate cortex multiplex information about reward and action. *J Neurosci* **30**: 3339-3346.
12. Amemori K, Graybiel AM (2012). Localized microstimulation of primate pregenual cingulate cortex induces negative decision-making. *Nat Neurosci* **15**: 776-785.
13. Amemori K, Amemori S, Graybiel AM (2015). Motivation and affective judgments differentially recruit neurons in the primate dorsolateral prefrontal and anterior cingulate cortex. *J Neurosci* **35**: 1939-1953.
14. Via E, Fullana MA, Goldberg X, Tinoco-González D, Martínez-Zalacaín I, Soriano-Mas C *et al.* (2018). Ventromedial prefrontal cortex activity and pathological worry in generalised anxiety disorder. *Br J Psychiatry* **213**: 437-443.
15. Kennedy SH, Konarski JZ, Segal ZV, Lau MA, Bieling PJ, McIntyre RS *et al.* (2007). Differences in brain glucose metabolism between responders to CBT and venlafaxine in a 16-week randomized controlled trial. *Am J Psychiatry* **164**: 778-788.
16. Fox MD, Buckner RL, White MP, Greicius MD, Pascual-Leone A (2012). Efficacy of transcranial magnetic stimulation targets for depression is related to intrinsic functional connectivity with the subgenual cingulate. *Biol Psychiatry* **72**: 595-603.
17. Roberts AC, Clarke HF (2019). Why we need nonhuman primates to study the role of ventromedial prefrontal cortex in the regulation of threat- and reward-elicited responses. *Proc Natl Acad Sci U S A*
18. Myers-Schulz B, Koenigs M (2012). Functional anatomy of ventromedial prefrontal cortex: implications for mood and anxiety disorders. *Mol Psychiatry* **17**: 132-141.
19. Stawicka ZM, Massoudi R, Horst NK, Koda K, Gaskin PLR, Alexander L *et al.* (2020). Ventromedial prefrontal area 14 provides opposing regulation of threat and reward-

elicited responses in the common marmoset. *Proc Natl Acad Sci U S A* **117**: 25116-25127.
20. Wallis CU, Cockcroft GJ, Cardinal RN, Roberts AC, Clarke HF (2019). Hippocampal Interaction With Area 25, but not Area 32, Regulates Marmoset Approach-Avoidance Behavior. *Cereb Cortex* **29**: 4818-4830.
21. Zeredo JL, Quah SKL, Wallis CU, Alexander L, Cockcroft GJ, Santangelo AM *et al.* (2019). Glutamate Within the Marmoset Anterior Hippocampus Interacts with Area 25 to Regulate the Behavioral and Cardiovascular Correlates of High-Trait Anxiety. *J Neurosci* **39**: 3094-3107.
22. Way BM, Laćan G, Fairbanks LA, Melega WP (2007). Architectonic distribution of the serotonin transporter within the orbitofrontal cortex of the vervet monkey. *Neuroscience* **148**: 937-948.
23. Goodman WK (2004). Selecting pharmacotherapy for generalized anxiety disorder. *J Clin Psychiatry* **65 Suppl 13**: 8-13.
24. Lesch KP, Bengel D, Heils A, Sabol SZ, Greenberg BD, Petri S *et al.* (1996). Association of anxiety-related traits with a polymorphism in the serotonin transporter gene regulatory region. *Science* **274**: 1527-1531.
25. Lemonde S, Turecki G, Bakish D, Du L, Hrdina PD, Bown CD *et al.* (2003). Impaired repression at a 5-hydroxytryptamine 1A receptor gene polymorphism associated with major depression and suicide. *J Neurosci* **23**: 8788-8799.
26. Strobel A, Gutknecht L, Rothe C, Reif A, Mössner R, Zeng Y *et al.* (2003). Allelic variation in 5-HT1A receptor expression is associated with anxiety- and depression-related personality traits. *J Neural Transm (Vienna)* **110**: 1445-1453.
27. Allen L, Dwivedi Y (2020). MicroRNA mediators of early life stress vulnerability to depression and suicidal behavior. *Mol Psychiatry* **25**: 308-320.
28. Lopez JP, Kos A, Turecki G (2018). Major depression and its treatment: microRNAs as peripheral biomarkers of diagnosis and treatment response. *Curr Opin Psychiatry* **31**: 7-16.
29. Huntzinger E, Izaurralde E (2011). Gene silencing by microRNAs: contributions of translational repression and mRNA decay. *Nat Rev Genet* **12**: 99-110.
30. Izaurralde E (2015). GENE REGULATION. Breakers and blockers—miRNAs at work. *Science* **349**: 380-382.
31. Geaghan M, Cairns MJ (2015). MicroRNA and Posttranscriptional Dysregulation in Psychiatry. *Biol Psychiatry* **78**: 231-239.
32. Yoshino Y, Dwivedi Y (2020). Non-Coding RNAs in Psychiatric Disorders and Suicidal Behavior. *Front Psychiatry* **11**: 543893.
33. Belzeaux R, Lin R, Turecki G (2017). Potential Use of MicroRNA for Monitoring Therapeutic Response to Antidepressants. *CNS Drugs* **31**: 253-262.
34. Roy B, Yoshino Y, Allen L, Prall K, Schell G, Dwivedi Y (2020). Exploiting Circulating MicroRNAs as Biomarkers in Psychiatric Disorders. *Mol Diagn Ther* **24**: 279-298.
35. Finkenwirth C, van Schaik C, Ziegler TE, Burkart JM (2015). Strongly bonded family members in common marmosets show synchronized fluctuations in oxytocin. *Physiol Behav* **151**: 246-251.
36. Miller CT, Freiwald WA, Leopold DA, Mitchell JF, Silva AC, Wang X (2016). Marmosets: A Neuroscientific Model of Human Social Behavior. *Neuron* **90**: 219-233.
37. Santangelo AM, Ito M, Shiba Y, Clarke HF, Schut EH, Cockcroft G *et al.* (2016). Novel Primate Model of Serotonin Transporter Genetic Polymorphisms Associated with Gene Expression, Anxiety and Sensitivity to Antidepressants. *Neuropsychopharmacology* **41**: 2366-2376.

38. Santangelo AM, Sawiak SJ, Fryer T, Hong Y, Shiba Y, Clarke HF *et al.* (2019). Insula serotonin 2A receptor binding and gene expression contribute to serotonin transporter polymorphism anxious phenotype in primates. *Proc Natl Acad Sci U S A* **116**: 14761-14768.
39. Alexander L, Gaskin PLR, Sawiak SJ, Fryer TD, Hong YT, Cockcroft GJ *et al.* (2019). Fractionating Blunted Reward Processing Characteristic of Anhedonia by Over-Activating Primate Subgenual Anterior Cingulate Cortex. *Neuron* **101**: 307-320.e6.
40. Alexander L, Wood CM, Gaskin PLR, Sawiak SJ, Fryer TD, Hong YT *et al.* (2020). Over-activation of primate subgenual cingulate cortex enhances the cardiovascular, behavioral and neural responses to threat. *Nat Commun* **11**: 5386.
41. Wallis CU, Cardinal RN, Alexander L, Roberts AC, Clarke HF (2017). Opposing roles of primate areas 25 and 32 and their putative rodent homologs in the regulation of negative emotion. *Proc Natl Acad Sci U S A* **114**: E4075-E4084.
42. Shiba Y, Santangelo AM, Braesicke K, Agustín-Pavón C, Cockcroft G, Haggard M *et al.* (2014). Individual differences in behavioral and cardiovascular reactivity to emotive stimuli and their relationship to cognitive flexibility in a primate model of trait anxiety. *Front Behav Neurosci* **8**: 137.
43. Carey GJ, Costall B, Domeney AM, Jones DN, Naylor RJ (1992). Behavioural effects of anxiogenic agents in the common marmoset. *Pharmacol Biochem Behav* **42**: 143-153.
44. Barros M, Boere V, Huston JP, Tomaz C (2000). Measuring fear and anxiety in the marmoset (Callithrix penicillata) with a novel predator confrontation model: effects of diazepam. *Behav Brain Res* **108**: 205-211.
45. Mobbs D, Headley DB, Ding W, Dayan P (2020). Space, Time, and Fear: Survival Computations along Defensive Circuits. *Trends Cogn Sci* **24**: 228-241.
46. Quah SKL, McIver L, Roberts AC, Santangelo AM (2020). Trait Anxiety Mediated by Amygdala Serotonin Transporter in the Common Marmoset. *J Neurosci* **40**: 4739-4749.
47. Lutz PE, Tanti A, Gasecka A, Barnett-Burns S, Kim JJ, Zhou Y *et al.* (2017). Association of a History of Child Abuse With Impaired Myelination in the Anterior Cingulate Cortex: Convergent Epigenetic, Transcriptional, and Morphological Evidence. *Am J Psychiatry* **174**: 1185-1194.
48. Krienen FM, Goldman M, Zhang Q, C H Del Rosario R, Florio M, Machold R *et al.* (2020). Innovations present in the primate interneuron repertoire. *Nature* **586**: 262-269.
49. Etkin A, Egner T, Peraza DM, Kandel ER, Hirsch J (2006). Resolving emotional conflict: a role for the rostral anterior cingulate cortex in modulating activity in the amygdala. *Neuron* **51**: 871-882.
50. Chang L, Zhou G, Soufan O, Xia J (2020). miRNet 2.0: network-based visual analytics for miRNA functional analysis and systems biology. *Nucleic Acids Res* **48**: W244-W251.
51. Li HJ, Qu N, Hui L, Cai X, Zhang CY, Zhong BL *et al.* (2020). Further confirmation of netrin 1 receptor (DCC) as a depression risk gene via integrations of multi-omics data. *Transl Psychiatry* **10**: 98.
52. Manitt C, Eng C, Pokinko M, Ryan RT, Torres-Berrío A, Lopez JP *et al.* (2013). dcc orchestrates the development of the prefrontal cortex during adolescence and is altered in psychiatric patients. *Transl Psychiatry* **3**: e338.
53. Torres-Berrío A, Lopez JP, Bagot RC, Nouel D, Dal Bo G, Cuesta S *et al.* (2017). DCC Confers Susceptibility to Depression-like Behaviors in Humans and Mice and Is Regulated by miR-218. *Biol Psychiatry* **81**: 306-315.

54. Torres-Berrío A, Hernandez G, Nestler EJ, Flores C (2020). The Netrin-1/DCC Guidance Cue Pathway as a Molecular Target in Depression: Translational Evidence. *Biol Psychiatry* **88**: 611-624.
55. Torres-Berrío A, Morgunova A, Giroux M, Cuesta S, Nestler EJ, Flores C (2020). miR-218 in Adolescence Predicts and Mediates Vulnerability to Stress. *Biol Psychiatry*
56. Torres-Berrío A, Nouel D, Cuesta S, Parise EM, Restrepo-Lozano JM, Larochelle P *et al.* (2020). MiR-218: a molecular switch and potential biomarker of susceptibility to stress. *Mol Psychiatry* **25**: 951-964.
57. Quah SKL, Cockcroft GJ, McIver L, Santangelo AM, Roberts AC (2020). Avoidant Coping Style to High Imminence Threat Is Linked to Higher Anxiety-Like Behavior. *Front Behav Neurosci* **14**: 34.
58. Oikonomidis L, Santangelo AM, Shiba Y, Clarke FH, Robbins TW, Roberts AC (2017). A dimensional approach to modeling symptoms of neuropsychiatric disorders in the marmoset monkey. *Dev Neurobiol* **77**: 328-353.
59. Wilkie MJ, Smith G, Day RK, Matthews K, Smith D, Blackwood D *et al.* (2009). Polymorphisms in the SLC6A4 and HTR2A genes influence treatment outcome following antidepressant therapy. *Pharmacogenomics J* **9**: 61-70.
60. Schaeffer DJ, Hori Y, Gilbert KM, Gati JS, Menon RS, Everling S (2020). Divergence of rodent and primate medial frontal cortex functional connectivity. *Proc Natl Acad Sci U S A* **117**: 21681-21689.
61. Ironside M, Amemori KI, McGrath CL, Pedersen ML, Kang MS, Amemori S *et al.* (2020). Approach-Avoidance Conflict in Major Depressive Disorder: Congruent Neural Findings in Humans and Nonhuman Primates. *Biol Psychiatry* **87**: 399-408.
62. Hodge RD, Bakken TE, Miller JA, Smith KA, Barkan ER, Graybuck LT *et al.* (2019). Conserved cell types with divergent features in human versus mouse cortex. *Nature* **573**: 61-68.
63. Issler O, van der Zee YY, Ramakrishnan A, Wang J, Tan C, Loh YE *et al.* (2020). Sex-Specific Role for the Long Non-coding RNA LINC00473 in Depression. *Neuron* **106**: 912-926.e5.
64. Lopez JP, Lim R, Cruceanu C, Crapper L, Fasano C, Labonte B *et al.* (2014). miR-1202 is a primate-specific and brain-enriched microRNA involved in major depression and antidepressant treatment. *Nat Med* **20**: 764-768.
65. Tessier-Lavigne M, Goodman CS (1996). The molecular biology of axon guidance. *Science* **274**: 1123-1133.
66. Srour M, Rivière JB, Pham JM, Dubé MP, Girard S, Morin S *et al.* (2010). Mutations in DCC cause congenital mirror movements. *Science* **328**: 592.
67. Rajman M, Schratt G (2017). MicroRNAs in neural development: from master regulators to fine-tuners. *Development* **144**: 2310-2322.
68. Schratt G (2009). Fine-tuning neural gene expression with microRNAs. *Curr Opin Neurobiol* **19**: 213-219.
69. Fiori LM, Kos A, Lin R, Théroux JF, Lopez JP, Kühne C *et al.* (2020). miR-323a regulates ERBB4 and is involved in depression. *Mol Psychiatry*
70. Lopez JP, Fiori LM, Cruceanu C, Lin R, Labonte B, Cates HM *et al.* (2017). MicroRNAs 146a/b-5 and 425-3p and 24-3p are markers of antidepressant response and regulate MAPK/Wnt-system genes. *Nat Commun* **8**: 15497.
71. Camkurt MA, Karababa İF, Erdal ME, Kandemir SB, Fries GR, Bayazıt H *et al.* (2020). MicroRNA dysregulation in manic and euthymic patients with bipolar disorder. *J Affect Disord* **261**: 84-90.

72. He C, Bai Y, Wang Z, Fan D, Wang Q, Liu X *et al.* (2021). Identification of microRNA-9 linking the effects of childhood maltreatment on depression using amygdala connectivity. *Neuroimage* **224**: 117428.
73. Maffioletti E, Cattaneo A, Rosso G, Maina G, Maj C, Gennarelli M *et al.* (2016). Peripheral whole blood microRNA alterations in major depression and bipolar disorder. *J Affect Disord* **200**: 250-258.
74. Bahi A, Dreyer JL (2018). Lentiviral-mediated let-7d microRNA overexpression induced anxiolytic- and anti-depressant-like behaviors and impaired dopamine D3 receptor expression. *Eur Neuropsychopharmacol* **28**: 1394-1404.
75. Ma ZY, Chen F, Xiao P, Zhang XM, Gao XX (2019). Silence of MiR-9 protects depression mice through Notch signaling pathway. *Eur Rev Med Pharmacol Sci* **23**: 4961-4970.
76. Zhang Y, Du L, Bai Y, Han B, He C, Gong L *et al.* (2020). CircDYM ameliorates depressive-like behavior by targeting miR-9 to regulate microglial activation via HSP90 ubiquitination. *Mol Psychiatry* **25**: 1175-1190.
77. Lopizzo N, Zonca V, Cattane N, Pariante CM, Cattaneo A (2019). miRNAs in depression vulnerability and resilience: novel targets for preventive strategies. *J Neural Transm (Vienna)* **126**: 1241-1258.
78. Zhou L, Zhu Y, Chen W, Tang Y (2021). Emerging role of microRNAs in major depressive disorder and its implication on diagnosis and therapeutic response. *J Affect Disord* **286**: 80-86.
79. Roberts AC (2020). Prefrontal Regulation of Threat-Elicited Behaviors: A Pathway to Translation. *Annu Rev Psychol* **71**: 357-387.
80. Labermaier C, Masana M, Müller MB (2013). Biomarkers predicting antidepressant treatment response: how can we advance the field. *Dis Markers* **35**: 23-31.

FIGURES AND FIGURE LEGENDS

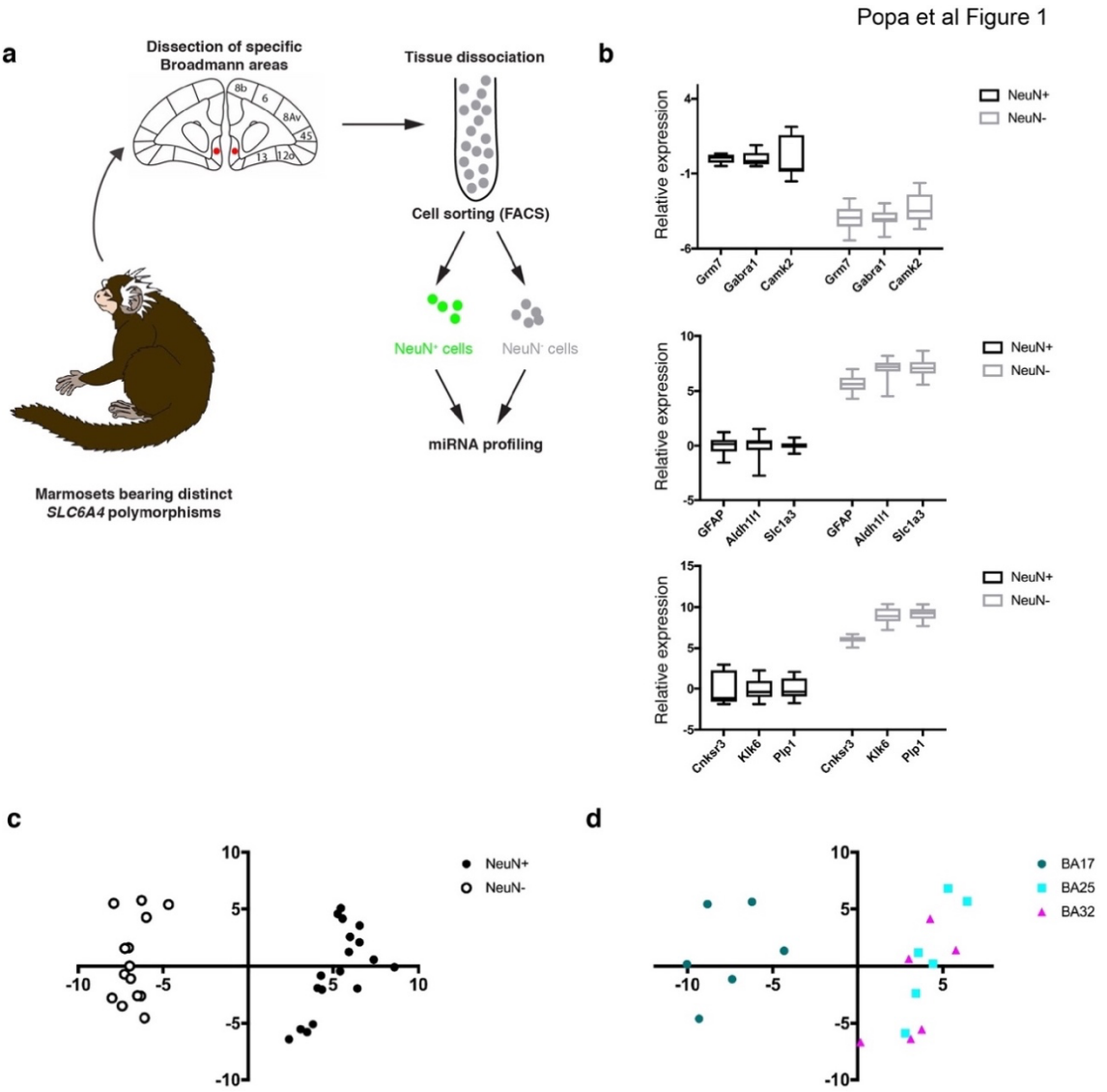

Figure 1. Schematic representation of experimental protocol and validation steps.

a) Experimental protocol included the genotypic and phenotypic characterization of the marmosets. After sacrifice, brains were frozen and sliced without fixation. RNA was extracted from punches of different cortical regions. Samples were subsequently submitted to nuclear isolation, NeuN staining and FACS sorting.

b) Expression of neuronal (top panel), astrocytic (middle panel) and oligodendrocytic (bottom panels) markers in $NeuN^+$ and $NeuN^-$ fractions confirmed the efficiency of the FACS sorting strategy.

c) PCA analysis on the levels of 92 miRNAs expressed in both $NeuN^+$ and $NeuN^-$ nuclei demonstrated that miRNAs profiles clearly differentiate both fractions.

d) PCA analysis on miRNAs level in $NeuN^+$ fraction enabled regional discrimination. Samples from the visual cortex clearly clustered apart from those of the vmPFC which, in turn, are intermingled.

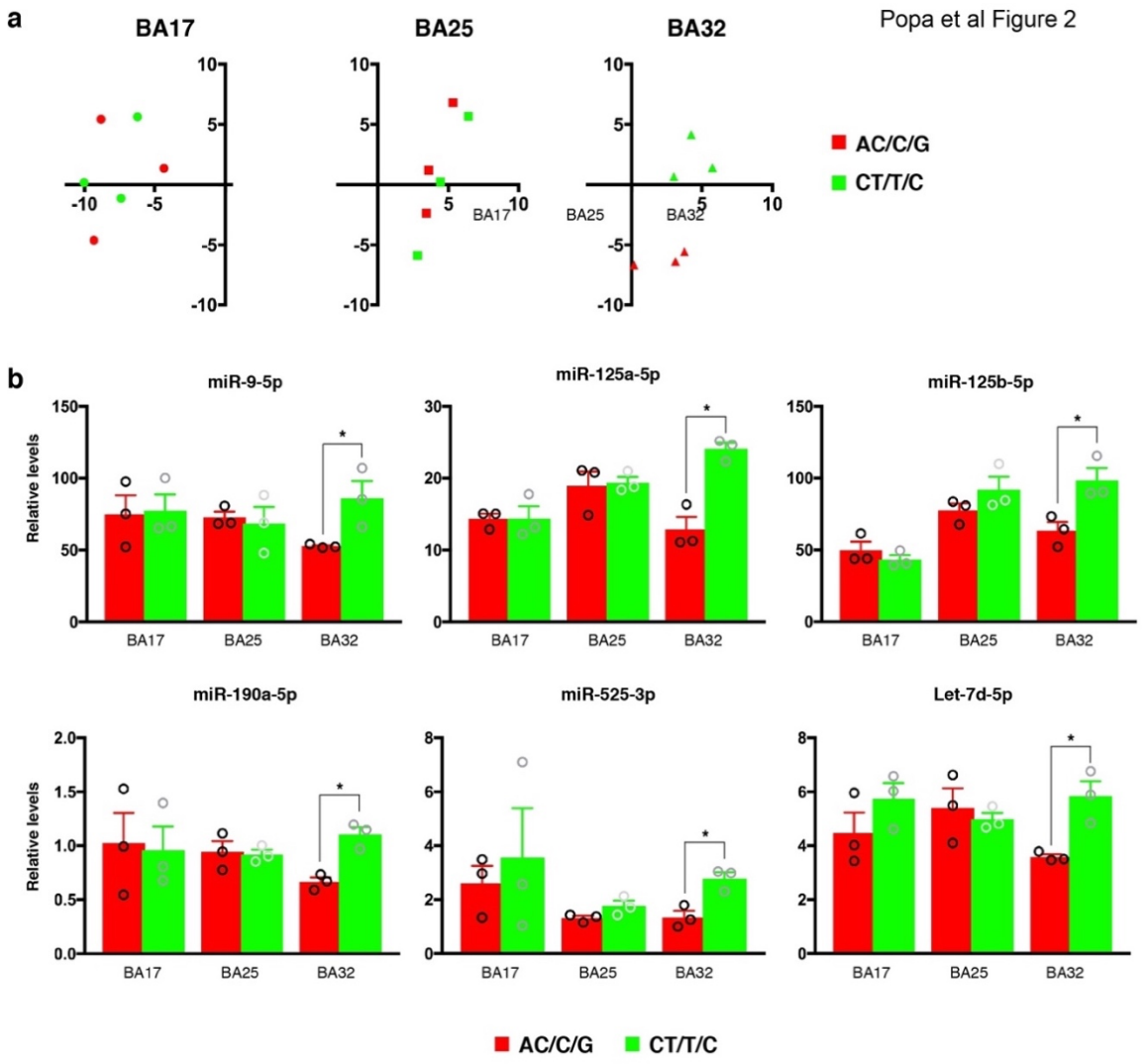

Figure 2. SLC6A4 polymorphisms (AC/C/G and CT/T/C) and miRNA signature in area 32.

a) PCA analysis on miRNAs level in NeuN^{+} nuclei showed genotypic differences only in area 32.

b) miRNAs differentially expressed in area 32 in AC/C/G and CT/T/C marmosets (One way ANOVA followed by Bonferroni's test for multiple comparisons, * p<.05).

Popa et al Figure 3

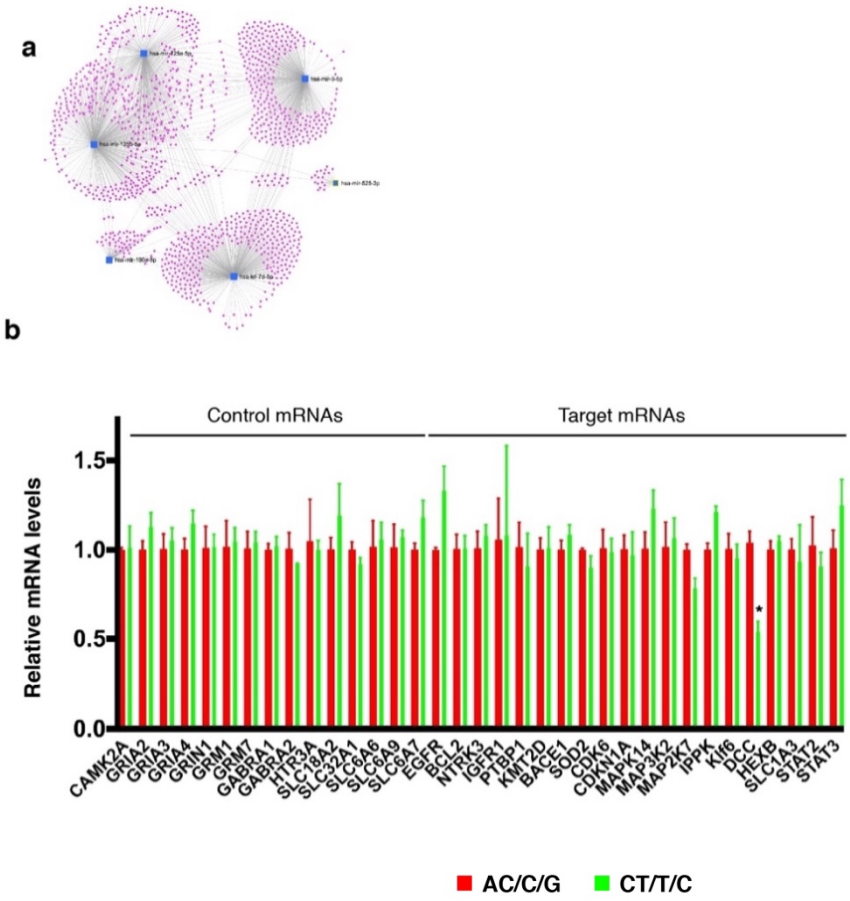

Figure 3. Expression of target mRNAs.

a) Network analysis using miRNAs deregulated in area 32.

b) Expression of target mRNAs identified by network analysis in area 32 and 25. Using as reference the AC/C/G genotype, we measured the abundance of 20 potential targets as well as 15 reference genes. Only Dcc was found to be differentially expressed in area 32 ($p=0.0483$, 2-way ANOVA followed by Tukey test for multiple comparisons, $p<0.05$)

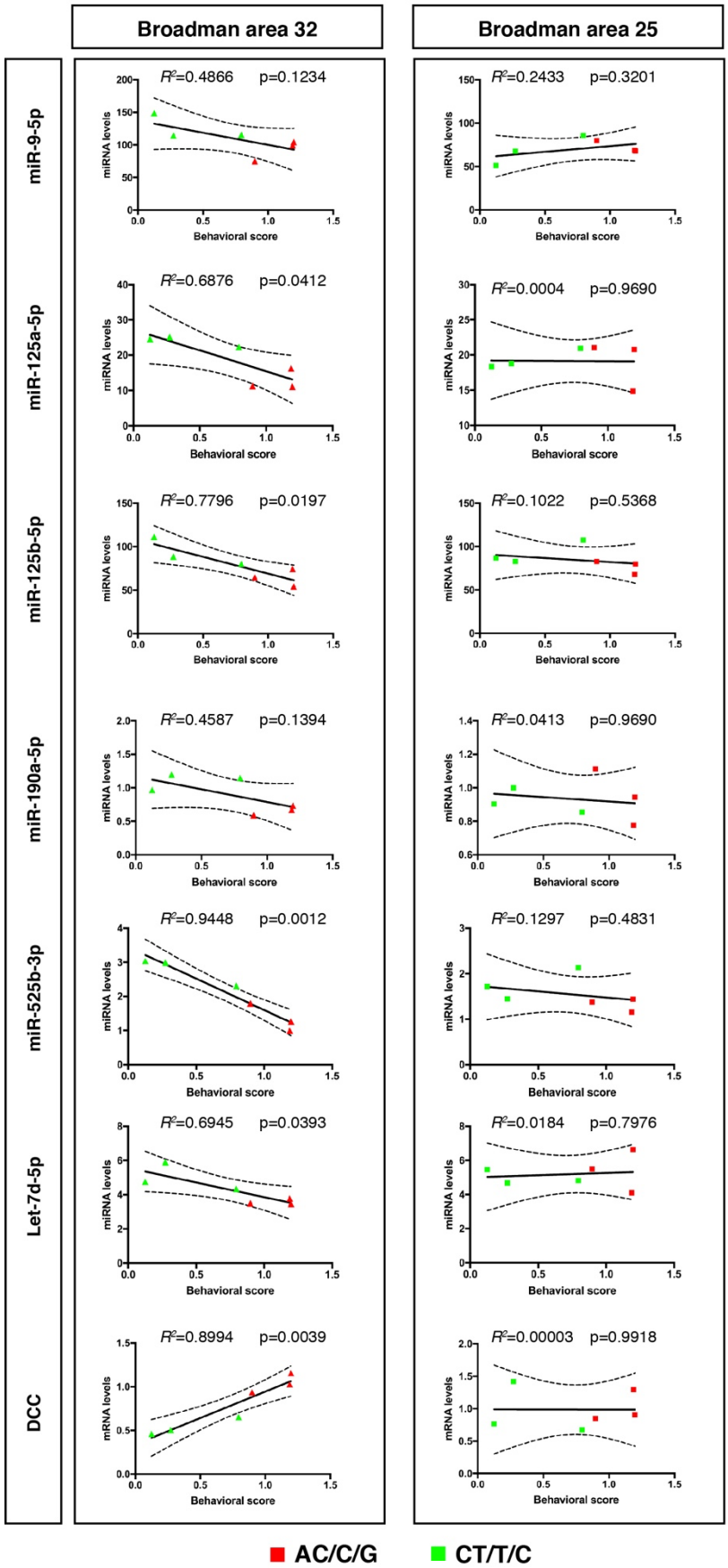

Figure 4. Correlation between miRNA and DCC levels in area 32 (left panels) or 25 (right panels) and behavioral response in the human intruder test.

Popa et al Figure 5

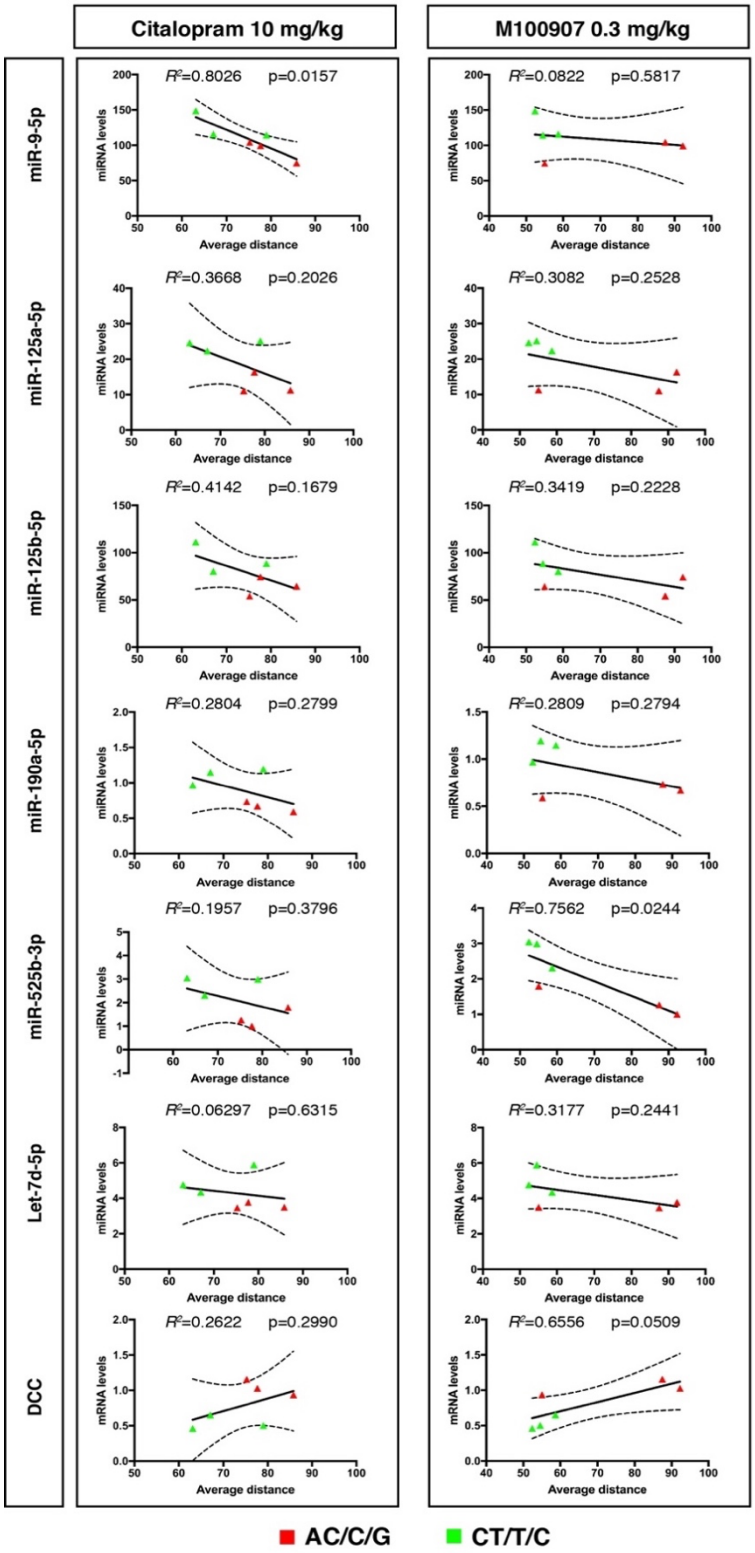

Figure 5. Correlation between miRNA and DCC levels in area 32 and average distance during the intruder phase after an acute injection of citalopram (left panels) or the 5-HT2a antagonist M100907 (right panels).

Table 1. Statistical analysis of expression levels of top 25 miRNAs from PCA (One-way ANOVA adjusted for multiple comparison with Bonferroni's correction).

miRNA	Area 25 (AC vs CT) Adjusted p value	Area 32 (AC vs CT) Adjusted p value
let-7a-5p	>0.999	0.1181
let-7d-5p	>0.999	**0.0208**
miR-9-5p	0.9891	**0.0475**
miR-26a-5p	>0.999	0.4908
miR-100-5p	0.2004	0.1486
miR-124-3p	0.3564	0.1234
miR-125a-5p	>0.999	**0.0013**
miR-125b-5p	0.4031	**0.0196**
miR-129-1-3p	0.2080	0.6278
miR-133a-5p	>0.999	0.8187
miR-144-3p	>0.999	>0.999
miR-190a-5p	>0.999	**0.0032**
miR-195-5p	>0.999	0.6839
miR-200a-3p	>0.999	0.1737
miR-221-3p	>0.999	>0.999
miR-222-3p	>0.999	0.4192
miR-302b-3p	0.2303	0.5073
miR-320a	0.9693	>0.999
miR-376a-3p	0.5647	>0.999
miR-378a-3p	>0.999	0.0554

miR-495-3p	>0.999	>0.999
miR-497-5p	0.9585	0.6780
miR-525-3p	0.3089	**0.0019**
miR-628-3p	>0.999	>0.999
miR-645	0.4508	>0.999

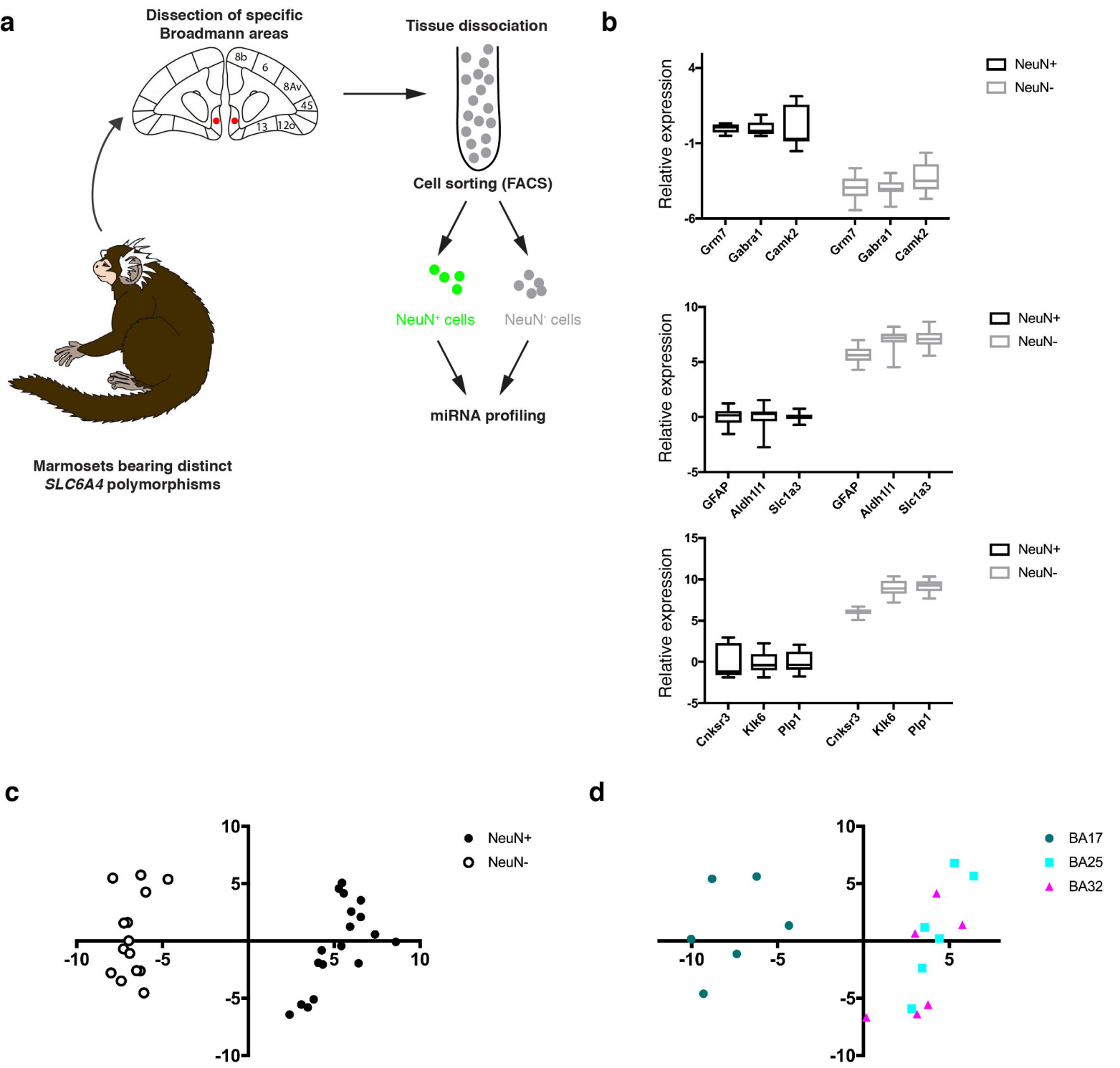

Figure 1. Schematic representation of experimental protocol and validation steps.
a) Experimental protocol include the genotypic and phenotypic characterization of the marmosets. After sacrifice, brains were frozen and sliced without fixation. RNA was extracted from punches of different cortical regions. Samples were previously submitted to nuclear isolation, NeuN staining and FACS sorting.
b) Expression of neuronal (top panel), astrocytic (middle panel) and oligodendrocytic (bottom panels) markers in NeuN$^+$ and NeuN$^-$ fractions confirms the efficiency of the FACS sorting strategy.
c) PCA analysis on the levels of 92 miRNAs expressed in both NeuN$^+$ and NeuN$^-$ nuclei demonstrate that miRNAs profiles clearly differentiate both fractions.
d) PCA analysis on miRNAs level in NeuN$^+$ fraction enables regional discrimination. Samples from the visual clearly cluster apart from those of the vmPFC which, in turn, are intermingled.

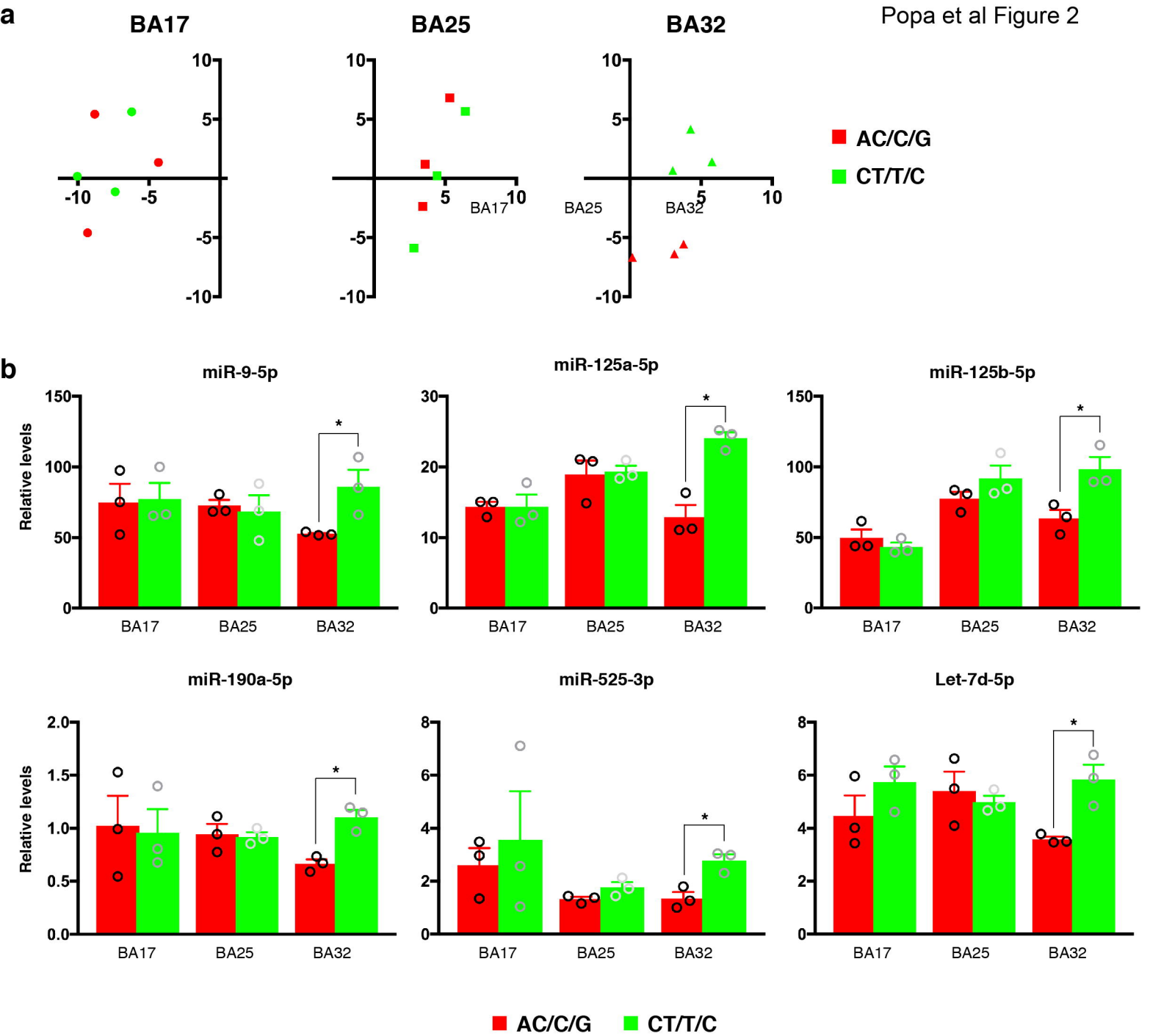

Figure 2. Slc6a4 polymorphisms (AC/C/G and CT/T/C) alter miRNA signature in area 32.
a) PCA analysis on miRNAs level in NeuN⁺ nuclei shows genotypic differences only in area 32.
b) Top miRNAs differentially expressed in area 32 in AC/C/G and CT/T/C marmosets (One way ANOVA fo llowed by Bonferroni's test for multiple comparisons, * $p<0.05$).

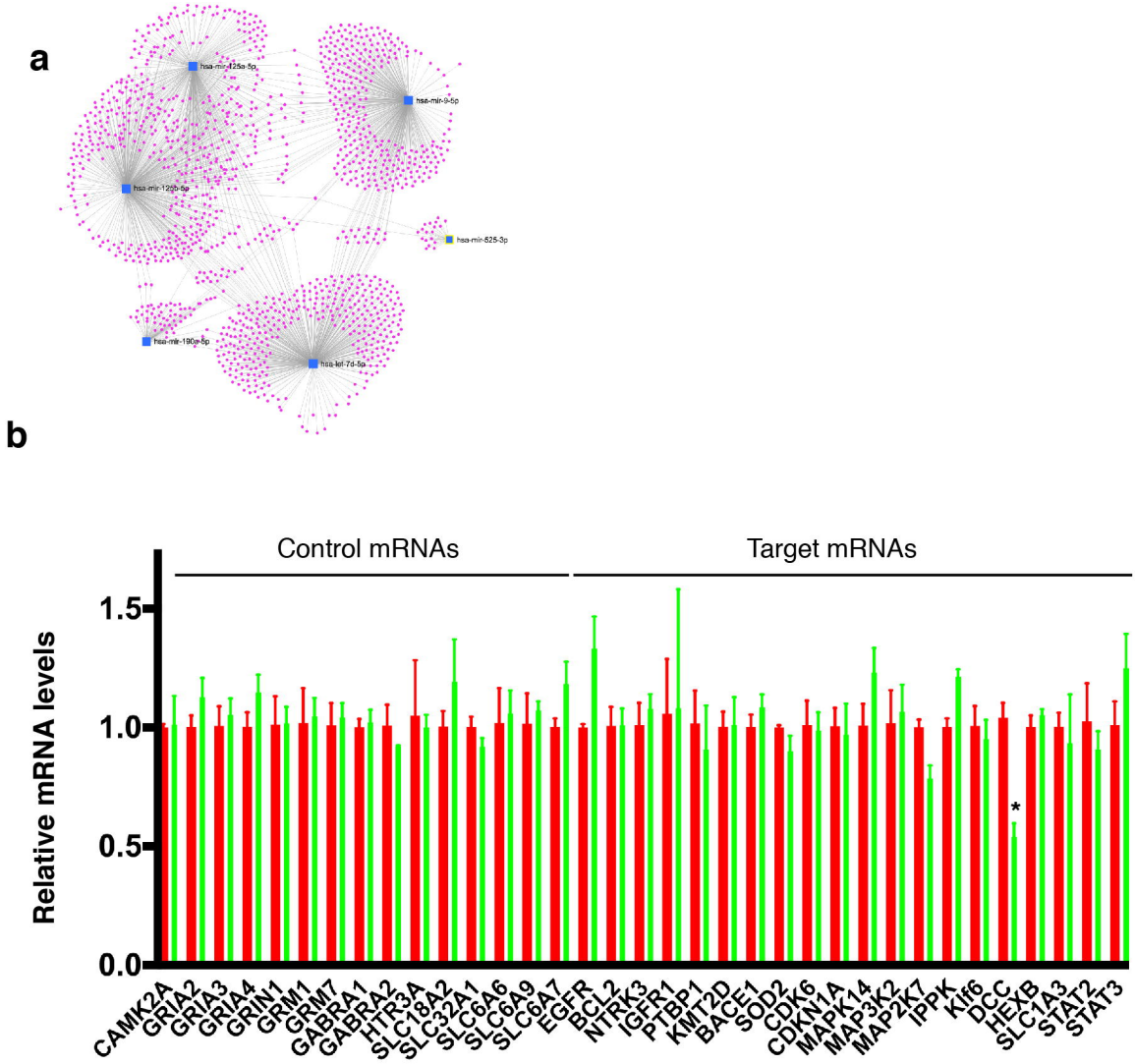

Figure 3. Target mRNAs in area 32.
a) Network analysis using miRNAs deregulated in area 32.
b) Expression of target mRNAs identified by network analysis in area 32. Using as reference the AC/C/G geno type, we measured the abundance of 20 potential targets as well as 15 reference genes. Only DCCwas found to be differentially expressed in area 32 (* $p<0.05$, t-test)

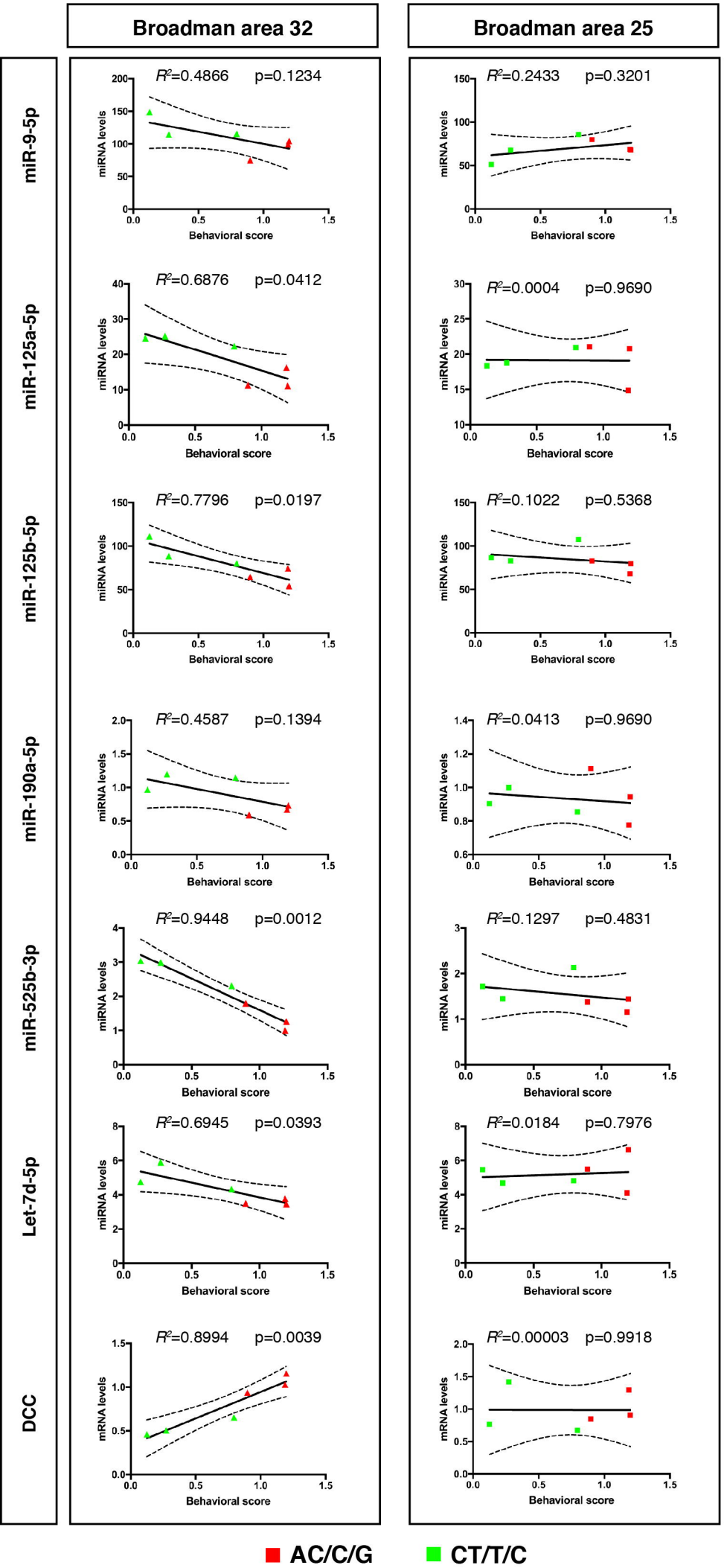

Figure 4. Correlation between miRNA and *DCC* levels in area 32 (left panels) or 25 (right panels) and behavioral response in the human intruder test.

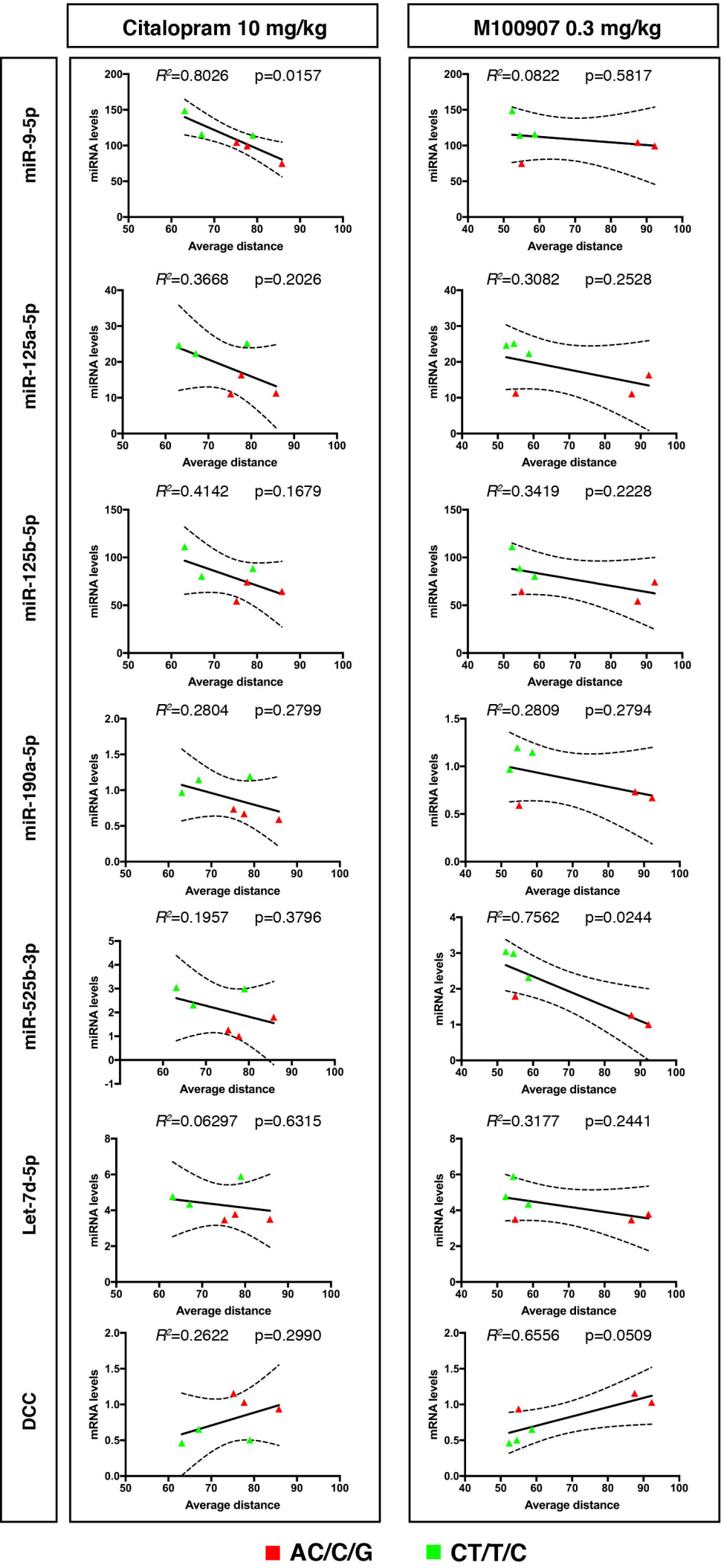

Figure 5. Correlation between miRNA and *DCC* levels in area 32 and average distance during the intruder phase after an acute injection of citalopram (left panels) or the 5-HT2a antagonist M100907 (right panels).